PROCEEDINGS OF SCIENCE

Dilepton production spectrum above T_c analyzed with a lattice quark propagator

Taekwang Kim*
Department of Physics, Osaka University, Toyonaka 560-0043, Japan
E-mail: kim@kern.phys.sci.osaka-u.ac.jp

Masayuki Asakawa
Department of Physics, Osaka University, Toyonaka 560-0043, Japan
E-mail: yuki@phys.sci.osaka-u.ac.jp

Masakiyo Kitazawa
Department of Physics, Osaka University, Toyonaka 560-0043, Japan
E-mail: kitazawa@phys.sci.osaka-u.ac.jp

We analyze the production rate of dileptons from the deconfined medium using a quark propagator obtained from a lattice QCD numerical simulation. We calculate the dilepton production rate non-perturbatively at two temperatures in the deconfined phase with the quark propagator obtained on the lattice. The photon-quark vertex is determined gauge-invariantly, so as to satisfy the Ward-Takahashi identity. The obtained dilepton production rate shows an enhancement of factor 10 or so compared with the rate from free quark systems at low invariant mass region and structure known as van Hove singularity.

9th International Workshop on Critical Point and Onset of Deconfinement - CPOD2014,
17-21 November 2014
ZiF (Center of Interdisciplinary Research), University of Bielefeld, Germany

*Speaker.

PoS(CPOD2014)057

1. INTRODUCTION

A deconfined medium is produced experimentally on the Earth by ultra-relativistic heavy ion collisions [1, 2]. The dilepton production is one of significant observables to study properties of the hot medium [3] because they penetrate and are unaffected by the medium. The dilepton production yield provides us direct information of the hot medium.

STAR and PHENIX Collaborations measured e^+e^- pair production yield at Relativistic Heavy Ion Collider (RHIC) at Brookhaven National Laboratory [4, 5]. Although the results of the pair production yields measured in the most central Au+Au collisions at $\sqrt{s_{NN}} = 200$ GeV reported by two collaborations do not coincide with each other, both of these Collaborations reported that the pair production yields show enhancements at low invariant mass, m, regions compared with the cocktail [4, 5, 6], The result of PHENIX Collaboration shows that the yeild for $m \simeq 500$ MeV is about one order larger than the cocktail, which implies that the medium modification effects significantly enhance the dilepton production rate.

When one performs an estimate of the dilepton production yield, one first calculates the dilepton production *rate* per unit time and unit volume from a static medium. The dilepton production rate of a static medium is proportional to the imaginary part of virtual photon self-energy [7, 8, 9]. When the temperature, T, is asymptotically high, the photon self-energy can be calculated perturbatively. Using the hard thermal loop (HTL) resummed perturbation theory [10, 11], the dilepton production rates are calculated in Ref. [12] for lepton pairs with zero total three-momentum, and the result is extended in Ref. [13] to nonzero momentum. It is, however, nontrivial whether or not such a perturbative analysis well describes the production rate from the deconfined medium near the critical temperature T_c, where the medium is turned out to be a strongly-coupled system [1]. It is therefore desirable to evaluate the dilepton production rate in the deconfined phase incorporating non-perturbative effects.

The exact non-perturbative photon self-energy can be calculated with the Schwinger-Dyson equation (SDE) if we have the full quark propagator and the photon-quark vertex function. Recently, an analysis of the non-perturbative quark propagator above T_c is performed on the lattice in the quenched approximation in Landau gauge [14, 15, 16] based on the two-pole ansatz. From the comparison with the perturbative analysis of the quark propagator [21, 22, 23, 24], it is expected that the quark propagator obtained in this simple ansatz well characterizes the non-perturbative nature of the quark propagator.

The purpose of the present study [25] is to analyze the dilepton production rate using this quark propagator. We construct the SDE with the quark propagator obtained on the lattice in Ref. [16] with the vertex function constructed so as to satisfy the Ward-Takahashi identity (WTI). Our formalism, therefore, fulfills the conservation law of electric current. In this analysis, we show that the obtained dilepton production rate exhibits an enhancement of one order larger than the one from free quark gas.

2. Schwinger-Dyson equation for photon self-energy

2.1 Schwinger-Dyson equation

As dileptons are emitted from decays of virtural photons, the dilepton production rate from a

medium per unit time per unit volume is related to the retarded self-energy $\Pi^R_{\mu\nu}(\omega,\vec{q})$ of the virtual photon as [7, 8, 9]

$$\frac{\mathrm{d}^4\Gamma}{\mathrm{d}\omega\mathrm{d}^3q} = \frac{\alpha}{12\pi^4}\frac{1}{Q^2}\frac{1}{\mathrm{e}^{\beta\omega}-1}\mathrm{Im}\Pi^{R,\mu}_{\mu}(\omega,\vec{q}), \tag{2.1}$$

at the leading order of fine structure constant α with $Q^2=\omega^2-\vec{q}^2$ and the inverse temperature $\beta=1/T$. With the SDE in Matsubara formalism, the exact photon self-energy is given by the full quark propagator $S(P)$ and full photon-quark vertex $\Gamma_\mu(P+Q,P)$ as

$$\Pi_{\mu\nu}(i\omega_m,\vec{q}) = -3\sum_f e_f^2 T\sum_n\int\frac{\mathrm{d}^3p}{(2\pi)^3}\mathrm{Tr}_D\left[S(P)\gamma_\mu S(P+Q)\Gamma_\nu(P+Q,P)\right], \tag{2.2}$$

where $\omega_m=2\pi Tm$ and $\nu_n=(2n+1)\pi T$ with integers m and n are the Matsubara frequencies for bosons and fermions, respectively, $P_\mu=(i\nu_n,\vec{p})$ is the four-momentum of a quark in the imaginary time, and e_f is the electric charge of a quark with an index f representing the quark flavor. Tr_D denotes the trace over Dirac indices, and the factor 3 in Eq. (2.2) comes from trace over color indices. The retarded photon self-energy is obtained by the analytic continuation

$$\Pi^R_{\mu\nu}(\omega,\vec{q}) = \Pi_{\mu\nu}(i\omega_m,\vec{q})|_{i\omega_m\to\omega+i\eta}. \tag{2.3}$$

In the following, we consider the two-flavor system with degenerate u and d quarks, where $\sum_f e_f^2 = 5e^2/9$. In this study we also limit our attention to $\vec{q}=0$ case.

2.2 Lattice Quark Propagator and Spectral Function

In the present study, we use the quark propagator obtained on the quenched lattice in Ref. [16] as the full quark propagator in Eq. (2.2). In this subsection, after a brief review on the general property of the quark propagator, we describe how to implement the results in Ref. [16] in our analysis.

On the lattice with a gauge fixing, one can measure the imaginary-time quark propagator

$$S^{aa}_{\mu\nu}(\tau,\vec{p}) = \int\mathrm{d}^3x\mathrm{e}^{-i\vec{p}\cdot\vec{x}}\langle\psi^a_\mu(\tau,\vec{x})\bar{\psi}^a_\nu(0,\vec{0})\rangle, \tag{2.4}$$

where $\psi^a_\mu(\tau,\vec{x})$ is the quark field with the Dirac index μ and the color index a. Here, τ is the imaginary time restricted to the interval $0\le\tau<\beta$. $S^{aa}_{\mu\nu}$ is a diagonal component, not traced out on the color indices. In the following section, the color indices of the quark field are suppressed in Eq. (2.4). The Fourier transform of the quark correlator

$$S_{\mu\nu}(i\nu_n,\vec{p}) = \int_0^\beta d\tau\mathrm{e}^{i\nu_n\tau}S_{\mu\nu}(\tau,\vec{p}), \tag{2.5}$$

is written in the spectral representation as

$$S_{\mu\nu}(i\nu_n,\vec{p}) = -\int\mathrm{d}\nu'\frac{\rho_{\mu\nu}(\nu',\vec{p})}{\nu'-i\nu_n}, \tag{2.6}$$

with the quark spectral function $\rho_{\mu\nu}(i\nu_n,\vec{p})$. The spectral function is related to the imaginary-time correlator Eq. (2.4) as

$$S_{\mu\nu}(\tau,\vec{p}) = \int_{-\infty}^{\infty}\mathrm{d}\nu\frac{\mathrm{e}^{(1/2-\tau/\beta)\beta\nu}}{\mathrm{e}^{\beta\nu/2}+\mathrm{e}^{-\beta\nu/2}}\rho_{\mu\nu}(\nu,\vec{p}). \tag{2.7}$$

In the deconfined phase, where the chiral symmetry is restored, the quark propagator anticommutes with γ_5. In this case, the spectral function can be decomposed with the projection operators $\Lambda_\pm(\vec{p}) = \left(1 \pm \gamma_0 \hat{\vec{p}} \cdot \vec{\gamma}\right)/2$ as

$$\rho(\nu, \vec{p}) = \rho_+(\nu, p)\Lambda_+(\vec{p})\gamma_0 + \rho_-(\nu, p)\Lambda_-(\vec{p})\gamma_0, \tag{2.8}$$

with $p = |\vec{p}|$, $\hat{\vec{p}} = \vec{p}/p$ and

$$\rho_\pm(\nu, p) = \frac{1}{2}\mathrm{Tr}_D\left[\rho\left(\nu, \vec{p}\right)\gamma_0\Lambda_\pm\left(\vec{p}\right)\right]. \tag{2.9}$$

It is shown from the anticommutation relations of ψ and $\bar{\psi}$ that the decomposed spectral functions satisfy the sum rule,

$$\int \mathrm{d}\nu \rho_\pm(\nu, p) = 1. \tag{2.10}$$

Using charge conjugation symmetry, one can show that $\rho_\pm(\nu, \vec{p})$ satisfy [16]

$$\rho_\pm(\nu, p) = \rho_\mp(-\nu, p). \tag{2.11}$$

On the lattice, one can measure the imaginary-time correlator Eq. (2.4) for discrete imaginary times. To obtain the quark propagator one has to deduce the spectral function from this information. In Refs. [14, 15, 16], the quark correlator in Landau gauge is analyzed on the lattice with the quenched approximation, and the quark spectral function is analyzed with the two-pole ansatz,

$$\rho_+(\nu, p) = Z_+(p)\delta\left(\nu - \nu_+(p)\right) + Z_-(p)\delta\left(\nu + \nu_-(p)\right), \tag{2.12}$$

where $Z_\pm(p)$ and $\nu_\pm(p)$ are the residues and positions of poles, respectively. Four parameters, $Z_\pm(p)$ and $\nu_\pm(p)$, are determined by fitting correlators obtained on the lattice for each p. The two poles in Eq. (2.12) at $\nu_+(p)$ and $\nu_-(p)$, respectively, correspond to the normal and plasmino modes in the HTL approximation. In fact, the study of the momentum and bare quark mass, m_0, dependences of the fitting paramters shows that these parameters behave reasonably as functions of m_0 and p [14, 15, 16]. The restoration of the chiral symmetry for massless quarks above T_c is also checked explicitly on the lattice by measuring of the scalar term of the massless quark propagator [15, 16].

In Fig. 1, we show the fitting result of each parameter in Eq. (2.12) for massless quarks as a function of p for $T = 1.5T_c$ and $3T_c$ obtained in Ref. [16]. These analyses are performed on the lattice with the size $128^3 \times 16$, at which both the lattice spacing and finite volume effects are found to be small [16]. In the upper panel, p dependences of $\nu_\pm(p)$, i.e. the dispersion relations of the normal and plasmino modes, are shown by open symbols. The vertical and horizontal axes are normalized by the thermal mass m_T defined by the value of $\nu_\pm(p)$ for $p = 0$. The value of m_T obtained on the lattice after the extrapolation to infinite volume limit is $m_T/T = 0.768(11)$ and $0.725(14)$ at $T = 1.5T_c$ and $3T_c$, respectively [16]. The lower panel shows the relative weight of the plasmino residue, $Z_-/(Z_+ + Z_-)$. The panel shows that the weight becomes smaller as p increases, which indicates that the quark propagator for large p/T is dominated by the normal mode.

Although the lattice data are available only for discrete values of p, we need to have the quark propagator as a continuous function of p to solve the SDE. For this purpose, we take interpolation and extrapolation of the lattice data by the cubic spline method. From the charge conjugation symmetry one can show that $d\nu_+(p)/dp = -d\nu_-(p)/dp$, $d^2\nu_+(p)/dp^2 = d^2\nu_-(p)/dp^2$, and

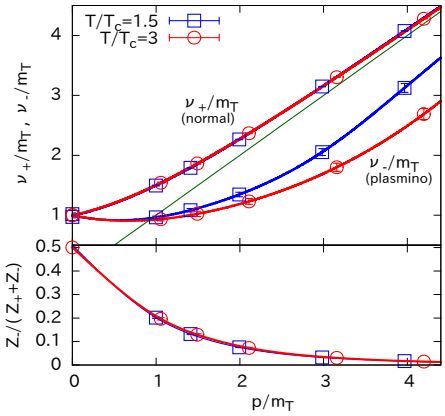

Figure 1: Open sympols show the momentum dependence of the parameters $\nu_+(p)$, $\nu_-(p)$, and $Z_-(p)/(Z_+(p)+Z_-(p))$ obtained on the lattice in Ref. [16]. The solid lines represent their interpolation obtained by the cubic spline method.

$Z_+(0) = Z_-(0)$ [14, 16]. These properties are taken into account in our cubic spline interpolation. The lattice data are available only in the momentum range $p/T \lesssim 4.7$. To take extrapolations to higher momenta, we extrapolate the parameters using an exponentially damping form for $Z_-/(Z_+ + Z_-)$, $Z_-/(Z_+ + Z_-) = \mathrm{e}^{-\alpha p}$, while $\nu_\pm(p)$ we extrapolate by a polynomial function, $\nu_\pm(p) = p + \beta_1^\pm/p + \beta_2^\pm/p^2 + \cdots$, which approach the light cone for large p with the parameters α and $\beta_i^\pm$ are determined in the cubic spline analysis. The p dependence of each parameter determined in this way is shown by the solid lines in Fig. 1. Finally, we demand $Z_+ + Z_- = 1$ throughout this paper to satisfy the sum rule Eq. (2.10).

With the two-pole form of the spectral function Eq. (2.12), the quark propagator reads

$$\begin{aligned} S(i\nu_n,\vec{p}) &= S_+(i\nu_n,p)\Lambda_+(\vec{p})\gamma_0 + S_-(i\nu_n,p)\Lambda_-(\vec{p})\gamma_0 \\ &= \sum_{s=\pm} S_s(i\nu_n,p)\Lambda_s(\vec{p})\gamma_0, \end{aligned} \tag{2.13}$$

where

$$S_s(i\nu_n,p) = \frac{Z_+(p)}{i\nu_n - s\nu_+(p)} + \frac{Z_-(p)}{i\nu_n + s\nu_-(p)} \tag{2.14}$$

with $s = \pm 1$. Correspondingly, the inverse propagator is given by

$$S^{-1}(i\nu_n,\vec{p}) = \sum_s S_s^{-1}(i\nu_n,p)(\vec{p})\gamma_0\Lambda_s(\vec{p}) \tag{2.15}$$

with

$$S_s^{-1}(i\nu_n,p) = \frac{(i\nu_n - s\nu_+(p))(i\nu_n + s\nu_-(p))}{i\nu_n - sE(p)}, \tag{2.16}$$

and $E(p) = -Z_+(p)\nu_-(p) + Z_-(p)\nu_+(p)$. Note that the inverse propagator has poles at $i\nu_n = \pm E$. This pole inevitably appears in the two-pole ansatz, because the propagator Eq. (2.14) has one zero

point in the range of ω sandwiched by the two poles. The form of the inverse propagator Eq. (2.16) will be used in the construction of the vetex function. We will see that the poles at $i\nu_n = \pm E$ give rise to additional terms in the dilepton production rate.

2.3 Vertex Function

The SDE Eq. (2.2) requires the full photon-quark vertex $\Gamma_\mu(P+Q,P)$ besides the full quark propagator. So far, the evaluation of $\Gamma_\mu(P+Q,P)$ on the lattice at nonzero temperature has not been performed to the best of the authors' knowledge. In the present study, we construct the vertex function from the lattice quark propagator to satisfy the Ward-Takahashi identity (WTI) as follows.

The gauge invariance requires that the vertex function fulfill the WTI

$$Q_\mu \Gamma^\mu(P+Q,P) = S^{-1}(P+Q) - S^{-1}(P), \tag{2.17}$$

with the inverse quark propagator $S^{-1}(P)$. For $\vec{q}=0$, the temporal component Γ_0 is completely determined only by this constraint as follows. First, in this case $\vec{q}\cdot\vec{\Gamma}$ should vanish provided that Γ_i is not singular at $\vec{q}=0$. Then, by substituting $\vec{q}\cdot\vec{\Gamma}=0$ into Eq. (2.17) one obtains

$$\Gamma_0(i\omega_m + i\nu_n, \vec{p}; i\nu_n, \vec{p}) = \frac{1}{i\omega_m}\left[S^{-1}(i\omega_m + i\nu_n, \vec{p}) - S^{-1}(i\nu_n, \vec{p})\right]. \tag{2.18}$$

On the other hand, the spatial components Γ_i cannot be determined only with Eq. (2.17) [17]. In the present study, we employ an approximation to neglect the $\vec{q}$ dependence of $\Gamma_0(i\omega_m + i\nu_n, \vec{p}+\vec{q}; i\nu_n, \vec{p})$ at $\vec{q}=0$; in other words we assume that

$$\partial\Gamma_0(i\omega_m + i\nu_n, \vec{p}+\vec{q}; i\nu_n, \vec{p})/\partial q_i|_{\vec{q}=0} = 0. \tag{2.19}$$

Within this approximaiton and Eq. (2.17), one obtains

$$q^i\Gamma_i(i\omega_m + i\nu_n, \vec{p}+\vec{q}; i\nu_n, \vec{p}) = S^{-1}(i\omega_m + i\nu_n, \vec{p}+\vec{q}) - S^{-1}(i\omega_m + i\nu_n, \vec{p}). \tag{2.20}$$

By taking the leading-order terms of $\vec{q}$ on the both sides, one obtains

$$\begin{aligned}\Gamma_i(i\omega_m + i\nu_n, \vec{p}; i\nu_n, \vec{p}) &= \frac{\partial S^{-1}}{\partial p^i}(i\omega_m + i\nu_n, \vec{p}) \\ &= \sum_s \frac{\partial S_s^{-1}(i\omega_m + i\nu_n, p)}{\partial p^i}\gamma_0\Lambda_s(\vec{p}) \\ &+ \sum_s S_s^{-1}(i\omega_m + i\nu_n, p)\gamma_0\frac{\partial\Lambda_s(\vec{p})}{\partial p^i},\end{aligned} \tag{2.21}$$

where in the second equality, we used Eq. (2.15).

The determination of the non-perturbative form of the photon-quark and gluon-quark vertices is generally difficult, and various approximations have been employed in the study with the SDE [17, 18, 19, 20]. It should be emphasized that the vertex functions Eqs. (2.18) and (2.21) satisfy the WTI and thus is advantageous in light of the gauge invariance among various ansätze on the vertex function. Eq. (2.18) is the same as that obtained in Ref. [17], since it is uniquely determined only from the WTI; while Γ_i are different from the ones in Ref. [17].

3. Dilepton production rate

Now, let us calculate the dilepton production rate with the lattice quark propagtor Eq. (2.13) and the full vertex functions Eqs. (2.18) and (2.21).

When the full vertex function satisfying the WTI is used in Eq. (2.2), the temporal component Π_{00} for $\vec{q}=0$ vanishes, because of the current conservation $q_\mu j^\mu = 0$. For $\sum_i \Pi_{ii}$, by substituting Eqs. (2.13) and (2.21) in Eq. (2.2) and using the two-pole form of the quark propagator Eq. (2.14) one obtains

$$\begin{aligned}\sum_i \Pi_{ii}\left(i\omega_m,\vec{0}\right) = &-\frac{10e^2}{3}\int\frac{\mathrm{d}^3p}{(2\pi)^3}\sum_{s=\pm1} s\left[\frac{2Z_+^2\nu_+\bar{\Omega}}{p(\nu_++E)}\frac{1-2f(\nu_+)}{i\omega_m+2s\nu_+}+\frac{2Z_-^2\nu_-\bar{\Omega}}{p(\nu_--E)}\frac{1-2f(\nu_-)}{i\omega_m+2s\nu_-}\right.\\
&+2Z_+Z_-\bar{\Omega}\frac{\bar{\Omega}E-2\omega_+\omega_-}{p(\nu_++E)(\nu_--E)}\frac{f(\nu_-)-f(\nu_+)}{i\omega_m-s\nu_++s\nu_-}\\
&-\left(Z_+\frac{\mathrm{d}\nu_-}{\mathrm{d}p}-Z_-\frac{\mathrm{d}\nu_+}{\mathrm{d}p}\right)\frac{1-f(\nu_+)-f(\nu_-)}{i\omega_m+s\nu_++s\nu_-}\\
&\left.+\left(-\frac{2Z_+Z_-E\Omega^2}{p(\nu_++E)(\nu_--E)}-\frac{\mathrm{d}E}{\mathrm{d}p}\right)\left(Z_+\frac{f(E)-f(\nu_+)}{i\omega_m+s\nu_+-sE}+Z_-\frac{f(-E)-f(\nu_-)}{i\omega_m+s\nu_-+sE}\right)\right],\end{aligned} \tag{3.1}$$

with $\bar{\Omega}=\nu_+-\nu_-$.

By taking the analytic continuation $i\omega_m\to\omega+i\eta$ and imaginary part, one obtains

$$\begin{aligned}\mathrm{Im}\Pi_\mu^{R,\mu}(\omega,\vec{0}) = &-\frac{20\alpha}{3}\int\mathrm{d}pp^2\left\{-\frac{2\bar{\Omega}}{p}\left[\frac{Z_+^2\nu_+}{\nu_++E}\{1-2f(\nu_+)\}\delta(\omega-2\nu_+)\right.\right.\\
&+\frac{Z_-^2\nu_-}{\nu_--E}\{1-2f(\nu_-)\}\delta(\omega-2\nu_-)\\
&\left.-Z_+Z_-\frac{\bar{\Omega}E-2\nu_+\nu_-}{(\nu_++E)(\nu_--E)}\{f(\nu_-)-f(\nu_+)\}\delta(\omega-\nu_++\nu_-)\right]\\
&+\left(Z_+\frac{\mathrm{d}\nu_-}{\mathrm{d}p}-Z_-\frac{\mathrm{d}\nu_+}{\mathrm{d}p}\right)\{1-f(\nu_+)-f(\nu_-)\}\delta(\omega-\nu_+-\nu_-)\\
&+\left(\frac{2Z_+Z_-E\Omega^2}{p(\nu_++E)(\nu_--E)}+\frac{\mathrm{d}E}{\mathrm{d}p}\right)\\
&\left.\times[Z_+\{1-f(-E)-f(\nu_+)\}\delta(\omega-\nu_++E)+Z_-\{f(-E)-f(\nu_-)\}\delta(\omega-\nu_--E)]\right\}\\
&+(\omega\to-\omega).\end{aligned} \tag{3.2}$$

Now let us inspect the physical meaning of each term in Eq. (3.2). From the δ-functions and thermal factors, one finds that the two terms in the first and second line represent the pair creation and annihilation processes of normal and plasmino modes, respectively. The third line corresponds to the Landau damping. The term in the fourth line in Eq. (3.2) can be interpreted as the pair annihilation and creation of a normal and a plasmino modes. This process appears as a consequence of the vertex correction. We note that a similar process exists in the formula obtained in the HTL perturbation [12]. Thus, the terms in the first four lines in Eq. (3.2) can be understood as

the decay, creation, and scattering processes of quark quasi-particles. We also note that the Landau damping of two normal and two plasmino modes does not exist in Eq. (3.2), because such a term can have a nonzero value only for $\omega = 0$ for $\vec{q} = 0$.

On the other hand, one cannot give such interpretations to the terms in the fifth and sixth lines in Eq. (3.2). From the δ-functions and the thermal factors, these terms seem to represent the decay and creation rates with a quasi-particle mode with the energy $\pm E$, which, however, does not exist in the quark propagtor Eq. (2.14). Mathematically, these terms come from the poles in the vertex function Eq. (2.21). The poles appear in the vertex function via the WTI, Eq. (2.17) and the fact that the analytic continuation of the propagator $S_s(i\nu_n, p)$ have zero points at energies $\pm E$. As discussed in Sec. 2.2, the zero points in $S_s(\omega, p)$ inevitably appear between the two poles in the two-pole form of the quark propagator Eq. (2.14).

Another remark on Eq. (3.2) is the sign of each term in Eq. (3.2). In Eq. (3.2), all terms are separately positive definite for $\omega > 0$ except for the one in the fourth line, which becomes negative for sufficiently large ω. The negative contribution of this term, however, is canceled out by the last term; the sum of the fourth and fifth lines is positive. The total dilepton production rate for $\omega > 0$ therefore is positive definite as it should be.

We finally comment on the limiting behaviors of Eq. (3.2). First, in our two-pole ansatz the quark propagator for massless free quarks is obtained by setting

$$Z_+(p) = 1, \quad Z_-(p) = 0, \quad \nu_+(p) = p. \tag{3.3}$$

Equation (3.2) thus should reproduce the photon self-energy of the free quark gas, when Eq. (3.3) is substituted into it. This can be explicitly checked as follows. By substituting $Z_- = 0$, all terms including Z_- vanishes. Since $E = -\nu_-$ for $Z_- = 0$, the thrid and fourth lines in Eq. (3.2) without including Z_- cancel out with each other without constraints on $\nu_-(p)$. Only the first term in Eq. (3.2) thus survives, which gives the free quark result. Second, our analysis on the dilepton production rate approaches the free quark one in the large ω limit, because the lattice quark propagator used in this study reproduces Eq. (3.3) at large momenta. This behavior will be checked in the next section.

4. Numerical results

Now let us examine the numerical results for the dilepton production rate obtained in the previous section. In Fig. 2(a), we present the ω dependence of the dilepton production rate for $T = 1.5T_c$. In the figure, we also plot the result without vertex correction together with the rates obtained by HTL perturbation [12] and free quark gas. The value of the thermal mass m_T is taken from the one determined on the lattice [16].

Figure 2(a) shows that the production rate with the lattice quark propagator have divergences at two energies $\omega/m_T = \omega_1/m_T \simeq 1.1$ and $\omega/m_T = \omega_2/m_T \simeq 1.8$. For $\omega < \omega_1$, the rate is about one order larger than the free quark one, and is almost the same order as the HTL result [12]. This large production rate at low ω might explain the enhancement of the experimentally-observed dilepton spectrum at PHENIX [4]. The rate has a discontinuity at $\omega = \omega_1$, and is significantly suppressed compared with the free quark one for $\omega_1 < \omega < \omega_2$. The rate has another discontinuity at $\omega = \omega_2$, above which the rate is consistent with the free quark one. In the dilepton rate without

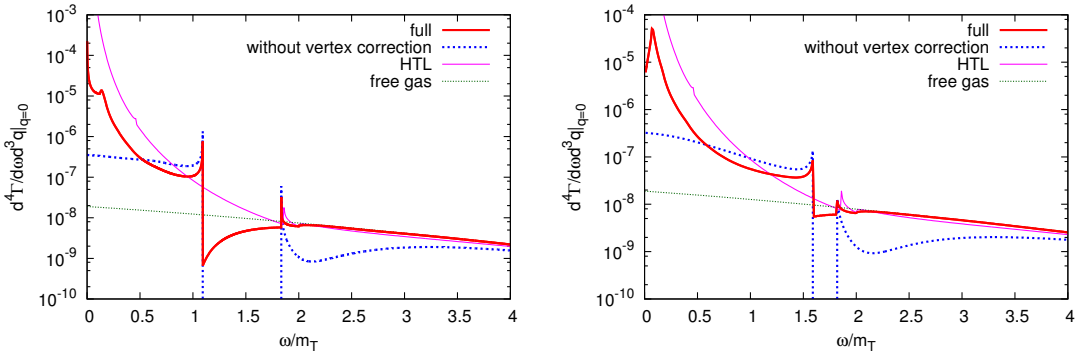

(a) $1.5T_c$ (b) $3T_c$

Figure 2: Dilepton production rates at zero momentum for $T = 1.5T_c$ and $3T_c$. The results without vertex correction are also plotted. Thin lines represent the HTL and free quark results.

vertex correction, one also finds two divergences at $\omega = \omega_1$ and ω_2, while the rate vanishes for $\omega_1 < \omega < \omega_2$.

In Fig. 2(b), we show the dilepton production rate at $T = 3T_c$. One sees that the behavior is qualitatively the same as the result for $T = 1.5T_c$. In particular, the rate is about one order larger than the free quark case for $\omega \simeq m_T$. This indicates that the large enhancement of the dilepton production rate around $\omega \simeq m_T$ is a general result for some range of T. Qualitatively, the gap between ω_1 and ω_2 becomes narrower, because of the change of the dispersion relations $\nu_\pm(p)$ obtained on the lattice. One also finds that the rate takes a finite value at $\omega = 0$, while it diverges for $T = 1.5T_c$. This limiting behavior strongly depends on the extrapolations of $\nu_\pm(p)$ to large momenta.

In this study we have investigated the dilepton production rate using a quark propagator obtained on the lattice with the two-pole ansatz. The Schwinger-Dyson equation (SDE) for the photon self-energy is solved with the lattice quark propagator and the photon-quark vertex satisfying the Ward-Takahashi identity. Our numerical result shows that the dilepton production rate with the lattice quark propagator is larger by the about one order at low invariant mass region compared with the free quark one. To understand the effect of the enhancement of the dilepton rate to the experimental result quantatively, analyses with dynamical models describing the space-time evolution of the hot medium are needed, which will be performed elsewhere.

T. K. is supported by Osaka University Cross-Boundary Innovation Program. This work is supported in part by JSPS KAKENHI Grant Numbers 26400272 and 25800148.

References

[1] I. Arsene *et al.* [BRAHMS Collaboration], Nucl. Phys. A **757**, 1 (2005) [nucl-ex/0410020]; B. B. Back, *et al.*, ibid. **757**, 28 (2005) [nucl-ex/0410022]; J. Adams *et al.* [STAR Collaboration], **757**, 102 (2005) [nucl-ex/0501009]; K. Adcox *et al.* [PHENIX Collaboration], **757**, 184 (2005) [nucl-ex/0410003].

[2] B. Muller, J. Schukraft and B. Wyslouch, Ann. Rev. Nucl. Part. Sci. **62**, 361 (2012) [arXiv:1202.3233 [hep-ex]].

[3] R. Rapp, J. Wambach and H. van Hees, arXiv:0901.3289 [hep-ph].

[4] A.Adare *et al.* [PHENIX Collaboration], Phys. Rev. C **81**, 034911 (2010)

[5] J. Zhao [STAR Collaboration], J. Phys. G **38**, 124134 (2011)

[6] L. Adamczyk *et al.* [STAR Collaboration], arXiv:1312.7397 [hep-ex].

[7] L. D. McLerran and T. Toimela, Phys. Rev. D **31**, 545 (1985).

[8] H. A. Weldon, Phys. Rev. D **42**, 2384 (1990).

[9] C. Gale and J. I. Kapusta, Nucl. Phys. B **357**, 65 (1991).

[10] E. Braaten and R. D. Pisarski, Nucl. Phys. B **337**, 569 (1990).

[11] R. D. Pisarski, Nucl. Phys. A **525**, 175 (1991).

[12] E. Braaten, R. D. Pisarski and T. -C. Yuan, Phys. Rev. Lett. **64**, 2242 (1990).

[13] S. M. H. Wong, Z. Phys. C **53**, 465 (1992).

[14] F. Karsch and M. Kitazawa, Phys. Rev. D **80**, 056001 (2009) [arXiv:0906.3941 [hep-lat]].

[15] M. Kitazawa and F. Karsch, Nucl. Phys. A **830**, 223C (2009) [arXiv:0908.3079 [hep-lat]].

[16] O. Kaczmarek, F. Karsch, M. Kitazawa and W. Soldner, Phys. Rev. D **86**, 036006 (2012) [arXiv:1206.1991 [hep-lat]].

[17] J. S. Ball and T. W. Chiu, Phys. Rev. D **22**, 2542 (1980).

[18] M. Harada, M. Kurachi and K. Yamawaki, Prog. Theor. Phys. **115**, 765 (2006) [hep-ph/0509193].

[19] F. Gao, S. X. Qin, Y. X. Liu, C. D. Roberts and S. M. Schmidt, Phys. Rev. D **89**, 076009 (2014) [arXiv:1401.2406 [nucl-th]].

[20] C. S. Fischer, J. Luecker and C. A. Welzbacher, Phys. Rev. D **90**, 034022 (2014) [arXiv:1405.4762 [hep-ph]].

[21] G. Baym, J. P. Blaizot and B. Svetitsky, Phys. Rev. D **46**, 4043 (1992).

[22] M. Kitazawa, T. Kunihiro and Y. Nemoto, Prog. Theor. Phys. **117**, 103 (2007) [hep-ph/0609164].

[23] M. Kitazawa, T. Kunihiro, K. Mitsutani and Y. Nemoto, Phys. Rev. D **77**, 045034 (2008) [arXiv:0710.5809 [hep-ph]].

[24] D. Satow, Y. Hidaka and T. Kunihiro, Phys. Rev. D **83**, 045017 (2011) [arXiv:1011.6452 [hep-ph]].

[25] T. Kim, M. Asakawa and M. Kitazawa, in preparation.